HHS Public Access

Author manuscript

Ann Neurol. Author manuscript; available in PMC 2018 April 02.

Published in final edited form as:

Ann Neurol. 2017 July ; 82(1): 67–78. doi:10.1002/ana.24974.

Connectivity Predicts Deep Brain Stimulation Outcome in Parkinson Disease

Andreas Horn, MD, PhD[1,2], **Martin Reich, MD**[3], **Johannes Vorwerk, PhD**[4], **Ningfei Li, M.Sc.**[5], **Gregor Wenzel, MD**[2], **Qianqian Fang, PhD**[6], **Tanja Schmitz-Hübsch, MD**[2,7], **Robert Nickl, MD**[8], **Andreas Kupsch, MD**[9,10], **Jens Volkmann, MD**[3], **Andrea A. Kühn, MD**[2,7], and **Michael D. Fox, MD, PhD**[1,11,12]

[1]Berenson-Allen Center for Noninvasive Brain Stimulation and Division of Cognitive Neurology, Department of Neurology, Beth Israel Deaconess Medical Center, Harvard Medical School, Boston, MA

[2]Department of Neurology, Movement Disorder and Neuromodulation Unit, Charité–Universitätsmedizin, Berlin, Germany

[3]Department of Neurology, Würzburg University Hospital, Würzburg, Germany

[4]Scientific Computing and Imaging Institute, University of Utah, Salt Lake City, Utah

[5]Institute of Software Engineering and Theoretical Computer Science, Neural Information Processing Group, Berlin Technical University, Berlin, Germany

[6]Department of Bioengineering, Northeastern University, Boston, MA

[7]NeuroCure Clinical Research Center, Charité–Universitätsmedizin, Berlin, Germany

[8]Department of Neurosurgery, Würzburg University Hospital, Würzburg, Germany

[9]Clinic of Neurology and Stereotactic Neurosurgery, Otto von Guericke University, Magdeburg, Germany

[10]Neurology Moves, Berlin, Germany

[11]Department of Neurology, Massachusetts General Hospital, Harvard Medical School, Boston, MA

[12]Athinoula A. Martinos Center for Biomedical Imaging, Charlestown, MA

Abstract

Address correspondence to Dr Fox and Dr Horn, Laboratory for Brain Network Imaging and Modulation, Berenson-Allen Center for Noninvasive Brain Stimulation, Department of Neurology, Beth Israel Deaconess Center, Harvard Medical School, 330 Brookline Avenue, Kirstein Building KS 158, Boston, MA 02215. mfox3@bidmc.harvard.edu, andreas.horn@charite.de.

Author Contributions

A.H., M.D.F., and A.A.K. contributed to the design of the study; A.H., M.D.F., A.A.K., M.R., J. Vor., Q.F., N.L., J. Vol., T.S.-H., A.K., G.W., and R.N. contributed to the acquisition and analysis of data; M.D.F., A.H., A.A.K., and M.R. contributed to drafting the text and preparing the figures. T.S.-H., J. Vol., A.K., J. Vor., Q.F., G.W., and R.N. reviewed and revised the manuscript for intellectual content.

Potential Conflicts of Interest

M.R., A.K., R.N., J. Vol., and A.A.K. have business relationships with Medtronics, St Judes, and Boston Scientific, which are makers of DBS devices, but none is related to the current work. M.D.F. has submitted a patent on using connectivity imaging to identify the ideal site for brain stimulation; the processing stream is different from this work.

Objective—The benefit of deep brain stimulation (DBS) for Parkinson disease (PD) may depend on connectivity between the stimulation site and other brain regions, but which regions and whether connectivity can predict outcome in patients remain unknown. Here, we identify the structural and functional connectivity profile of effective DBS to the subthalamic nucleus (STN) and test its ability to predict outcome in an independent cohort.

Methods—A training dataset of 51 PD patients with STN DBS was combined with publicly available human connectome data (diffusion tractography and resting state functional connectivity) to identify connections reliably associated with clinical improvement (motor score of the Unified Parkinson Disease Rating Scale [UPDRS]). This connectivity profile was then used to predict outcome in an independent cohort of 44 patients from a different center.

Results—In the training dataset, connectivity between the DBS electrode and a distributed network of brain regions correlated with clinical response including structural connectivity to supplementary motor area and functional anticorrelation to primary motor cortex ($p<0.001$). This same connectivity profile predicted response in an independent patient cohort ($p<0.01$). Structural and functional connectivity were independent predictors of clinical improvement ($p<0.001$) and estimated response in individual patients with an average error of 15% UPDRS improvement. Results were similar using connectome data from normal subjects or a connectome age, sex, and disease matched to our DBS patients.

Interpretation—Effective STN DBS for PD is associated with a specific connectivity profile that can predict clinical outcome across independent cohorts. This prediction does not require specialized imaging in PD patients themselves.

Deep brain stimulation (DBS) is a well-established treatment for Parkinson disease (PD), yielding improvements in motor symptoms and quality of life.[1] The most common DBS target is the subthalamic nucleus (STN), identified based on stereotactic coordinates and preoperative magnetic resonance imaging (MRI). However, the therapeutic benefit of DBS may depend on modulation of remote brain regions connected to the stimulation site.[2–4] These remote effects of DBS have been measured with both electrophysiology[5,6] and brain imaging.[3,7–10] Furthermore, they can correlate with clinical response.[11] As such, connectivity of the stimulation site to a network of other brain regions may be an important mediator of DBS response. If so, one could potentially predict response based on connectivity with the stimulation site and even optimize the DBS target based on connectivity.

Motivated by these findings, researchers have worked to determine which connections with the DBS site are most important. For example, the hyperdirect pathway connecting STN to cortex is thought to play a key role.[8,12–14] However, identifying connectivity noninvasively in humans is not straightforward. Two MRI-based connectivity measures appear promising. Diffusion tractography, a noninvasive metric of anatomical connectivity, can identify white matter tracts near the DBS electrode. [9,10,15–17] Functional connectivity, a measure of the correlation in spontaneous activity, can link DBS sites to cortical regions including targets of noninvasive brain stimulation.[2,18] Despite these efforts, the connectivity profile of clinically effective STN stimulation for PD remains unclear.

Here, we use high-quality connectome datasets of both diffusion tractography and functional connectivity to compute the connectivity profile of effective STN stimulation for PD. Most analyses used connectome data from normal subjects (n = 1,030), but we ensured results were reproducible using a connectome from PD patients (n = 90). Although group connectome data have not previously been used to study DBS outcomes, it has proven valuable in similar contexts.[2,19–25] We studied 2 large cohorts of PD patients with STN DBS (n = 51 and n = 44) to test the hypotheses that connectivity profiles predict clinical outcome across independent datasets.

Subjects and Methods

Patient Cohorts and Imaging

Ninety-five DBS patients from 2 different centers were retrospectively included in this study (mean age = 60.2 ± 8.0 years, 29 women). The first "training" dataset was from Charité–Universitätsmedizin, Berlin, whereas the second "test" dataset was from Würzburg University Hospital (Table). The study was carried out in accordance with the Declaration of Helsinki and was approved by the internal review board of Charité–Universitätsmedizin or Würzburg University Hospital (see below).

All patients (both datasets) underwent DBS surgery for PD and received 2 quadripolar DBS electrodes (model 3389; Medtronic, Minneapolis, MN). All patients received preoperative MRI and neuropsychological testing to exclude structural or severe psychiatric comorbidities. During surgery, microelectrode recordings were performed to verify lead placement. Clinical variables, including age, sex, disease duration before surgery, L-dopa response (percentage improvement on Unified Parkinson Disease Rating Scale [UPDRS]-III ON vs OFF) before surgery and L-dopa equivalent dose (LEDD) at baseline, were recorded and tested for predictive value of clinical outcome in a univariate analysis.

The Berlin (training) dataset consisted of 4 subcohorts, enrolled at different times and for different studies. These subcohorts were intentionally heterogenous in clinical presentation and DBS effects to ensure that results from this training dataset would be as generalizable as possible. One subcohort consisted of early stage PD patients (B_1), 1 subcohort was retrospectively gathered from medical records with only clinical assessment of UPDRS response (B_2), 1 subcohort consisted of a typical, average-aged study population of patients stimulated to the STN (B_3), and 1 subcohort had DBS targeting the nearby caudal zona incerta rather than the STN itself (B_4). Detailed clinical results of this final cohort will be reported elsewhere. For all patients in the Berlin cohort, DBS response was measured as percentage change in UPDRS motor score ON versus OFF DBS assessed 1 to 2 years postoperatively.

The Würzburg (test) dataset consisted of a single clinical cohort. DBS response was measured as percentage change in UPDRS motor score comparing postoperative ON DBS to preoperative baseline. Note that the DBS outcome measure was different in the Würzburg versus Berlin cohorts, which was intentional to ensure generalizability of our results. All UPDRS-III scores (both datasets) were recorded after withdrawal from dopaminergic medication for > 12 hours.

DBS Lead Localization

The DBS localization protocol largely followed the one described in Horn and Kühn[26] with some modifications. Briefly, postoperative images were linearly coregistered to preoperative MRI using SPM12 (http://www.fil.ion.ucl.ac.uk/spm/software/spm12/; postoperative MRI) or BRAINSFit software (https://www.nitrc.org/projects/multimodereg/; postoperative computed tomography). Coregistrations were manually controlled for each patient and refined if needed.

Images were then normalized into ICBM 2009b NLIN asymmetric space using the SyN approach implemented in advanced normalization tools (http://stnava.github.io/ANTs/) based on the preoperative MRI. DBS electrode contacts were localized within MNI space using Lead-DBS software (www.lead-dbs.org;[26]).

Volume of Tissue Activated Estimation

Volume of tissue activated (VTA) estimation largely followed the concepts described in McIntyre et al[27] and Åström et al[28] but processes were reimplemented using a novel open-source pipeline explained below. To construct a volume conductor model of the DBS electrode and surrounding tissue, a tetrahedral volume mesh was generated based on the surface meshes of DBS electrodes and subcortical nuclei using the Iso2Mesh toolbox (http://iso2mesh.sourceforge.net/) as included within Lead-DBS. Regions filled with neither conducting/insulating electrode material nor gray matter were assigned to white matter. Subcortical gray matter nuclei were defined by the DISTAL atlas.[29] Conductivities of 0.33 and 0.14S/m were assigned to gray and white matter, respectively.[30] For the platinum/iridium contacts and insulated parts of the electrodes, values of 10^{8}S/m and 10^{-16}S/m were used, respectively. Based on the volume conductor model, the potential distribution resulting from DBS was simulated using the integration of the FieldTrip-SimBio pipeline into Lead-DBS (https://www.mrt.uni-jena.de/simbio/index.php/; http://fieldtriptoolbox.org). The voltage applied to the active electrode contacts was introduced as a boundary condition. In case of monopolar stimulation, the surface of the volume mesh served as the anode. Subsequently, the gradient of the potential distribution was calculated by derivation of the finite element method (FEM) solution. Due to the first order FEM approach that was used, the resulting gradient is piecewise continuous. The gradient was thresholded for magnitudes above a commonly used value of 0.2V/mm[28,31] to define the extent and shape of the volume of tissue activated.

Connectivity Estimation

Functional and structural connectivity estimates between each VTA and all other brain voxels were computed using 2 connectomes: a large normative connectome from healthy subjects (n = 1,030) and a smaller connectome that was age, sex, and disease matched to our DBS patients (n = 90).

NORMATIVE CONNECTOME—Resting state functional connectivity data was obtained on 1,000 healthy subjects using a 3T Siemens (Erlangen, Germany) MRI, part of the Brain Genomics Superstruct Project (https://dataverse.harvard.edu/dataverse/GSP).[32] Processing included global signal regression and spatial smoothing at 6mm full width at half maximum

as previously described.[32] For structural connectivity, a group connectome was computed based on multishell diffusion-weighted (DSI Studio, http://dsi-studio.labsolver.org) and T2-weighted imaging data from 32 subjects of the Human Connectome Project at Massachusetts General Hospital (https://ida.loni.usc.edu/login.jsp). These data were acquired on a specially designed MRI scanner with more powerful gradients than available on conventional MRI scanners. Whole brain tractography fiber sets were calculated using a generalized q-sampling imaging algorithm as implemented in DSI Studio. Sampling was performed within a white matter mask that was defined using the unified segmentation approach on T2-weighted structural acquisitions and that was coregistered to the b_0 volume using SPM12. In each subject, 200,000 fibers were sampled. Fiber tracts were then transformed into MNI space as previously described.[24,33–35]

PD CONNECTOME—MRI data from 90 patients were obtained from the Parkinson's Progression Markers Initiative (PPMI) database (mean age = 61.38 ± 10.42 standard deviation, 28 female). This dataset was also age and sex matched to our full cohort (69% vs 68% women, difference in mean age = 1 year). Detailed scanning parameters can be found on the project website (www.ppmi-info.orgz). All 90 patients had diffusion-weighted scans, but only 74 had resting-state functional MRI scans. Processing of both functional and structural data was performed identical as in healthy subjects.

Connectivity between each VTA and voxels in the rest of the brain was estimated using the above connectome datasets. For functional connectivity, time series were sampled from voxels inside each VTA in each of the 1,000 (healthy)/74 (parkinsonian connectome) subjects and correlated with time series from every other voxel in the brain. These functional connectivity estimates were then averaged across subjects within the connectome dataset. For structural connectivity, fibers traversing through the VTA were selected from the group connectome and projected to the volumetric space of the brain in 2mm isotropic resolution, denoting the number of fibers (connected to the VTA) that traversed through each voxel.

Generating Models of Beneficial Connectivity

A map of gray matter voxels was defined by thresholding the tissue probability map supplied with SPM12 ($p > 0.2$, 2×2×2mm MNI-152 space). The (structural and functional) connectivity from VTAs to each voxel in this volume was calculated for each patient. Functional connectivity strength was expressed as averaged R values across the 1,000 subjects. Structural connectivity strength was expressed as numbers of fiber tracts between VTA and cortical voxels. Functional connectivity maps were Fisher z-transformed before performing spatial correlations. Likewise, structural connectivity profiles were transformed into a Gaussian distribution following the approach of van Albada.[36] Neither transformation (Fisher z or van Albada approach) altered main results reported in this article. Figure 1 summarizes methods to identify DBS connectivity.

We used our training dataset to evaluate different options for identifying connections predictive of clinical outcome. First, the connectivity map of each VTA was weighted by clinical improvement (*weighted average* maps). Second, voxels whose VTA connectivity was correlated with clinical outcome were identified (*R maps*). Third, we created maps of

voxels both connected to the VTA and correlated with clinical outcome (*combined maps)*. This third map was computed by masking the weighted average maps by the R maps ($R > 0$ for positive values and $R<0$ for negative values). Finally, we computed maps using either our normative connectome or our PD connectome.

To determine which option was best for predicting clinical outcome, we used our training dataset ($B_{1–4}$) and a leave-one-cohort out design. For example, we used cohorts B_1–B_3 to generate each of the above maps, then used the map to predict clinical outcome in cohort B_4. Clinical outcome estimates were based on the similarity between the "ideal" connectivity profile and the connectivity profile from each individual patient (measured using a Fisher *z*-transformed spatial correlation coefficient). This was done independently for structural and functional connectivity. The best model for predicting results across cohorts in the Berlin dataset ($B_{1–4}$) was then applied to the independent Würzburg test data (W).

Finally, we used the combined dataset ($B_{1–4} + W$; n = 95), and a general linear model (GLM) combining both structural and functional connectivity profiles to test (1) whether the 2 types of connectivity are independent predictors for clinical outcome and (2) how much of the outcome variance can be explained by the 2 connectivity measures combined. An initial GLM was computed based on connectivity estimates alone, whereas a second GLM included relevant baseline clinical variables.

To test how robustly outcome of individual patients could be predicted, the same GLMs were solved in a leave-one-patient-out fashion. In other words, data from 94 patients were used to predict the 95th patient and predicted improvement was compared to the actual improvement. The average prediction error was reported and 3 index patients were selected to show example results.

Results

Our DBS cohort included 95 patients across 2 independent datasets (30 female, mean age = 60.2 ± 8.0 years), 68 akinetic-rigid, 19 mixed, and 8 tremor-dominant cases (see Table). Average disease duration was 11.4 ± 4.3 years, baseline UPDRS score was 43.7 ± 13.4, L-dopa response was 57.6 ± 18.2%, and UPDRS improvement with DBS was 47.2 ± 22.4%. Reduction in LEDD comparing baseline to 12 months post-DBS was 58.3 % (1,250.0 ± 595.5 before vs 530.7 ± 389.2 after surgery). DBS response was heterogeneous across the Berlin subcohorts, which was intentional to ensure results would be robust to cohort differences.

Baseline UPDRS score was the only clinical variable predictive of DBS response in both the Berlin ($R = 0.33$, $p<0.02$) and Würzburg ($R = 0.35$, $p<0.02$) cohorts, with higher baseline scores predicting greater percentage improvement. Age at surgery ($R = –0.42$, $p = 0.002$) and female sex ($t = 2.5$, $p = 0.01$) were predictive in the Berlin but not the Würzburg cohort ($p > 0.8$ for both variables). Disease duration ($p > 0.4$), baseline L-dopa response ($p > 0.15$), and baseline LEDD ($p > 0.1$) were not predictive of DBS outcome in either cohort.

DBS lead placement was roughly similar across our 2 cohorts (Fig 2). Using patient-specific electrode locations and VTAs within the Berlin cohort (n = 51), we identified numerous

functional and structural connections correlated with clinical improvement (Fig 3). The better a patient's DBS connectivity profile matched these maps, the better their clinical outcome. This held true both on the full Berlin dataset (B_{1-4}) and in a leave-one-subcohort out fashion (eg, using B_{1-3} to estimate response in B_4). Several options for computing these connectivity maps were explored within the training dataset (see Subjects and Methods). The healthy connectome data and the combined maps (overlap of the weighted maps and R maps) explained the greatest variance in the leave-one-subcohort out analysis.

These connectivity profiles (combined maps, normative connectome) derived using the Berlin data were then used to predict clinical outcome in the independent Würzburg data (Fig 4). Both structural connectivity ($R = 0.45$, $p = 0.002$) and functional connectivity ($R = 0.34$, $p = 0.03$) were significant predictors of clinical outcome in this independent dataset despite differences in center, surgeon, and timing of clinical assessment.

Topography of connectivity to effective DBS sites (combined maps) was highly similar when computed for the Berlin training dataset (n = 51), Würzburg test dataset (n = 44), and full dataset (n = 95; Fig 5). Anticorrelation between DBS electrodes and primary motor cortex (M1), as well as structural connectivity to supplementary motor area (SMA), superior frontal gyrus, and cerebellum, was predictive of beneficial outcome in both datasets alone and the combined dataset.

Both structural ($p<0.006$) and functional ($p<0.007$) connectivity were independent predictors of clinical outcome. A combined model incorporating both types of connectivity explained 26.2% of the clinical variance in DBS response (correlation between predicted and true improvements of $R = 0.51$ at $p<10^{-8}$). Adding clinical variables to this model (age, sex, and UPDRS at baseline) explained 43.4% of the variance in DBS response ($R = 0.66$ at $p<10^{-13}$). In this final model, structural connectivity, functional connectivity, UPDRS at baseline, and sex were all significant independent predictors of DBS response ($p<0.05$).

In a final analysis, we explored how well we could predict outcome in individual patients based on connectivity of a patient's DBS electrode. This was done on the combined ($B_{1-4}+W$) dataset while leaving out the patient in question. These predictions on average deviated by 15.7 ± 14.2% from actual UPDRS-III improvements. For example, if a patient actually improved by 30%, our connectivity algorithm might predict an improvement of 45% or 15%. Including additional clinical variables (UPDRS at baseline, age at surgery, sex) to the analysis added little to the clinical predictions based on connectivity alone (mean error = 15.1 ± 11.8%). Three patients selected to illustrate a good responder with an accurate prediction, a poor responder with an accurate prediction, and a poor responder with an inaccurate prediction are shown in Figure 6.

Although our normative connectome performed slightly better than our PD connectome in our Berlin leave-one-subcohort out analysis, there is intuitive appeal to using an age-, sex-, and disease-matched connectome. We therefore repeated all analyses using this PD connectome and found results were highly similar. For example, functional connectivity between the VTA and M1 was highly correlated across patients using the normative versus PD connectome ($R = 0.97$, $p<10^{-7}$) and predicted similar variance in DBS response ($R =$

0.23, $p<0.05$ for normative vs $R = 0.17$, $p<0.05$ for PD). Likewise, structural connectivity between the VTA and SMA was highly correlated across patients using either connectome ($R = 0.80$, $p<10^{-7}$) and predicted similar variance in DBS response ($R = 0.27$, $p<0.005$ for normative vs $R = 0.21$, $p<0.05$ for PD). Finally, using the PD versus normative connectome to generate maps in the Berlin cohort and predict outcome in the Würzburg cohort gave similar results, both for functional connectivity ($R = 0.34$, $p<0.03$ for normative vs $R = 0.44$, $p<0.005$ for PD) and for structural connectivity ($R = 0.45$, $p<0.002$ for normative vs $R = 0.38$, $p<0.011$ for PD).

Discussion

Four main conclusions may be drawn from this study. First, a specific pattern of structural and functional connectivity with STN DBS electrodes correlates with clinical outcome across patients in PD. Second, structural and functional connectivity are independent predictors of DBS response. Third, connectivity profiles derived from one patient cohort can predict clinical outcome in an independent cohort from a different DBS center. Finally, we illustrate the potential of how connectivity profiles may be used to estimate outcome in single patients.

The Connectivity Profile of Effective STN DBS

There are 3 major differences between the current study and prior work examining the connectivity profile of effective DBS, both for PD[16] and for other disorders. [9,10,15,17] First, prior work focused on anatomical connectivity alone, whereas the current study included both anatomical and functional connectivity. Anatomical connectivity (based on diffusion MRI) has higher spatial resolution than functional connectivity (based on fMRI) and is thus more likely to identify differences between adjacent electrode contacts in the same patient. [8,16] However, when predicting outcome across different patients with variability in electrode location, our data suggest that functional connectivity adds predictive value above and beyond anatomical connectivity. This is consistent with other work.[25,33]

Second, the current study used previously collected connectome data rather than connectivity data from the individual patients enrolled in the study. Connectivity profiles of each DBS electrode were thus dependent on the position, size, and shape of the corresponding VTA only. This is a major practical advantage, as MRI-based connectivity data are not routinely acquired in DBS patients. As such, the current study could utilize large DBS cohorts across different centers (n = 95), whereas prior studies requiring patient-specific connectivity have been much smaller (n<25; Accolla et al,[8] Vanegas Arroyave et al[16]). The present approach may prove particularly valuable for emerging DBS indications with a limited number of patients implanted at different centers and heterogeneity in clinical response.[2,4,24,37] Such DBS datasets may be analyzed retrospectively even if no individual connectivity data were acquired.

An interesting question is which connectome dataset is best for identifying the connectivity profile of effective DBS. Normative connectomes from healthy subjects have the advantage of large subject numbers, excellent signal to noise ratio, and acquisition using unique high-power MRI scanners specifically designed for connectivity imaging. Such normative

connectome data have proven valuable in predicting stroke symptoms from patient-specific lesions,[19–23] and the present study shows its value in predicting clinical outcome from patient-specific electrodes. In contrast, patient-based connectomes have the advantage of better matching the connectivity of our DBS patients. Both prior work[2,25] and the current results show that results are similar using normative versus patient-based connectomes. Finally, acquiring connectivity data in each patient provides the best sensitivity to individual differences, but the lowest signal to noise ratio. It is worth noting that our results are broadly consistent with a prior study of STN DBS based on patient-specific connectivity.[16] Future work is needed to determine how to best combine the strengths of normative connectomes, patient-based connectomes, and connectivity data from individual patients.

One final difference between the current study and prior work relates to our focus on reproducibility across datasets. We utilized independent cohorts from different DBS centers, and intentionally selected heterogeneous cohorts to ensure reproducibility. Our cohorts were operated on by different surgeons, had different postoperative imaging, and had DBS response measured in different ways. Such heterogeneity could be seen as a limitation, as it decreases our power for detecting significant results. However, that our results were significant despite this heterogeneity is a major strength and should lead to improved reproducibility in other cohorts. To our knowledge, this is the first DBS imaging study to test for reproducibility of results across independent and heterogeneous cohorts.

Multimodal Confirmation

The connectivity profiles identified in the current study are consistent with prior work in PD patients using various modalities to identify brain regions modulated by STN DBS.[11] Brain regions anatomically connected and positively correlated with effective STN electrodes in the current study (eg, SMA, anterior cingulate, medial prefrontal cortex) have shown increased activity in neuroimaging studies when STN DBS is turned on.[7] The activation of SMA in particular is hypothesized to occur via activation of fibers within the hyperdirect pathway. [8,13] Atrophy in SMA and premotor cortex was also a predictor of DBS outcome in PD.[38] Our results confirm the importance of the SMA and to a lesser extent premotor and other frontal areas in DBS response.[5,8]

In contrast to the SMA, M1 was negatively correlated with effective STN DBS electrodes in the current study. Patients with a good response had DBS electrodes that were (functionally) negatively correlated to M1. Correspondingly, if DBS is activated, M1 has been reported to show decreased activity on neuroimaging.[7] These results suggest that functional connectivity may predict the sign of metabolic changes induced by DBS. Other work implicating M1 in the pathophysiology of PD includes abnormal connectivity between STN and M1[39] and modulation of M1 excitability by STN DBS.[40]

Implications for Network-Targeted Stimulation

By showing that connectivity predicts the response of individual PD patients to DBS, the current results support the notion that targets of therapeutic brain stimulation may be brain networks and not individual brain regions.[2,4,9,10,14–17] As such, different network nodes may potentially be targeted by different stimulation modalities with similar therapeutic benefit.

To that end, it is worth highlighting that connectivity of DBS electrodes to the 2 transcranial magnetic stimulation (TMS) targets shown to improve motor symptoms in PD, the SMA and M1, seems predictive of DBS effect in our study.[41,42] These cortical maps could help refine cortical TMS targets [2,25] or serve as the basis for multifocal arrays that can stimulate a distributed network.[43]

Predicting and Guiding DBS

That the current connectivity profiles were robust enough to predict DBS outcome across cohorts and DBS centers leads to the question of whether these connectivity profiles may have clinical utility. For example, in patients with unsatisfactory DBS response,[44] the current algorithm may help determine whether response is appropriate to electrode location (possibly requiring lead revision) or due to other potentially treatable factors. For instance, an index patient with poor DBS outcome for whom our model predicted good improvement (see Fig 6, bottom row) improved to match our prediction after being treated for severe depression on ward.[45] This case illustrates the potential of our approach, but also that many factors other than connectivity influence DBS response, including age, baseline severity of PD, L-dopa responsiveness, and disease subtype.[38,45–47] Despite these factors, our purely connectivity-based model explained 26% of the variance in motor outcome. Adding additional clinical variables further increased the amount of variance explained by our model to 44%. Interestingly, L-dopa responsiveness was not a predictor of DBS outcome in our study, consistent with other recent work.[47] Whether additional clinical or imaging variables will predict additional variance remains to be tested.

Limitations

Limitations of our study include heterogeneity between subcohorts of our training dataset. However, this was intentional to ensure results were robust to cohort differences. Second, the current analysis used a widely accepted VTA model.[28,31] However, more advanced VTA modeling approaches exist that could further improve our results.[48,49] Finally, our study was not designed to contrast the predictive ability of connectivity with anatomy (ie, electrode/VTA location[48,50]. No prior study has shown that anatomical location alone can predict DBS outcome in an independent cohort, but that does not mean that anatomy would not have been predictive in our case. Future work is needed to understand the relative contribution of anatomical location and connectivity to predicting outcome.

Acknowledgments

The study was supported by the Prof. Klaus Thiemann Foundation (A.H.), Stiftung Charité (A.H.), Berlin Institute of Health (A.H.), Deutsche Forschungsgemeinschaft (KFO247, A.A.K.), NIH National Institute of Neurological Disorders and Stroke (K23NS083741, M.D.F.), and Dystonia Medical Research Foundation (M.D.F.). M.R. was funded by a grant from IZKF of Würzburg University Hospital (Z-2/64), and Q.F. by the NIH/NIGMS (R01-GM114365). J. Vor. was funded by National Science Foundation US Ignite (10037840).

Data collection and sharing for this project were provided by the Human Connectome Project (HCP; principal investigators: Bruce Rosen, MD, PhD, Arthur W. Toga, PhD, Van J. Weeden, MD). HCP funding was provided by the NIH National Institute of Dental and Craniofacial Research, National Institute of Mental Health, and National Institute of Neurological Disorders and Stroke. HCP data are disseminated by the Laboratory of Neuro Imaging at the University of Southern California. HCP is the result of efforts of coinvestigators from the University of Southern California, Martinos Center for Biomedical Imaging at Massachusetts General Hospital, Washington University, and University of Minnesota.

Data used in the preparation of this article were obtained from the PPMI database (www.ppmi-info.org/data). For up-to-date information on the study, visit www.ppmi-info.org. PPMI, a public–private partnership, is funded by the Michael J. Fox Foundation for Parkinson's Research. For funding partners, see www.ppmi-info.org/fundingpartners.

We thank G.-H. Schneider for crucial help in data acquisition and analysis.

References

1. Schuepbach WMM, Rau J, Knudsen K, et al. Neurostimulation for Parkinson's disease with early motor complications. N Engl J Med. 2013; 368:610–622. [PubMed: 23406026]
2. Fox MD, Buckner RL, Liu H, et al. Resting-state networks link invasive and noninvasive brain stimulation across diverse psychiatric and neurological diseases. Proc Natl Acad Sci. 2014; 111:E4367–E4375. [PubMed: 25267639]
3. Henderson JM. "Connectomic surgery": diffusion tensor imaging (DTI) tractography as a targeting modality for surgical modulation of neural networks. Front Integr Neurosci. 2012; 6:15. [PubMed: 22536176]
4. Lozano AM, Lipsman N. Probing and regulating dysfunctional circuits using deep brain stimulation. Neuron. 2013; 77:406–424. [PubMed: 23395370]
5. Litvak V, Jha A, Eusebio A, et al. Resting oscillatory corticosubthalamic connectivity in patients with Parkinson's disease. Brain. 2011; 134(pt 2):359–374. [PubMed: 21147836]
6. Oswal A, Jha A, Neal S, et al. Analysis of simultaneous MEG and intracranial LFP recordings during deep brain stimulation: a protocol and experimental validation. J Neurosci Methods. 2016; 261:29–46. [PubMed: 26698227]
7. Ceballos-Baumann AO, Boecker H, Bartenstein P, et al. A positron emission tomographic study of subthalamic nucleus stimulation in Parkinson disease: enhanced movement-related activity of motor-association cortex and decreased motor cortex resting activity. Arch Neurol. 1999; 56:997–1003. [PubMed: 10448806]
8. Accolla EA, Herrojo Ruiz M, Horn A, et al. Brain networks modulated by subthalamic nucleus deep brain stimulation. Brain. 2016; 139(pt 9):2503–2515. [PubMed: 27412387]
9. Pouratian N, Zheng Z, Bari AA, et al. Multi-institutional evaluation of deep brain stimulation targeting using probabilistic connectivity-based thalamic segmentation. J Neurosurg. 2011; 115:995–1004. [PubMed: 21854118]
10. Riva-Posse P, Choi KS, Holtzheimer PE, et al. Defining critical white matter pathways mediating successful subcallosal cingulate deep brain stimulation for treatment-resistant depression. Biol Psychiatry. 2014; 76:963–969. [PubMed: 24832866]
11. Asanuma K, Tang C, Ma Y, et al. Network modulation in the treatment of Parkinson's disease. Brain. 2006; 129(pt 10):2667–2678. [PubMed: 16844713]
12. Gradinaru V, Mogri M, Thompson KR, et al. Optical deconstruction of parkinsonian neural circuitry. Science. 2009; 324:354–359. [PubMed: 19299587]
13. Nambu A, Tokuno H, Takada M. Functional significance of the cortico-subthalamo-pallidal "hyperdirect" pathway. Neurosci Res. 2002; 43:111–117. [PubMed: 12067746]
14. Haynes WIA, Haber SN. The organization of prefrontal-subthalamic inputs in primates provides an anatomical substrate for both functional specificity and integration: implications for basal ganglia models and deep brain stimulation. J Neurosci. 2013; 33:4804–4814. [PubMed: 23486951]
15. Coenen VA, Allert N, Mädler B. A role of diffusion tensor imaging fiber tracking in deep brain stimulation surgery: DBS of the dentato-rubro-thalamic tract (drt) for the treatment of therapy-refractory tremor. Acta Neurochir (Wien). 2011; 153:1579–1585. [PubMed: 21553318]
16. Vanegas Arroyave N, Lauro PM, Huang L, et al. Tractography patterns of subthalamic nucleus deep brain stimulation. Brain. 2016; 139(pt 4):1200–1210. [PubMed: 26921616]
17. Schlaepfer TE, Bewernick BH, Kayser S, et al. Deep brain stimulation of the human reward system for major depression—rationale, outcomes and outlook. Neuropsychopharmacology. 2014; 39:1303–1314. [PubMed: 24513970]

18. Anderson JS, Dhatt HS, Ferguson MA, et al. Functional connectivity targeting for deep brain stimulation in essential tremor. AJNR Am J Neuroradiol. 2011; 32:1963–1968. [PubMed: 21885716]
19. Fasano A, Laganiere SE, Lam S, Fox MD. Lesions causing freezing of gait localize to a cerebellar functional network. Ann Neurol. 2017; 81:129–141. [PubMed: 28009063]
20. Boes AD, Prasad S, Liu H, et al. Network localization of neurological symptoms from focal brain lesions. Brain. 2015; 138:3061–3075. [PubMed: 26264514]
21. Darby R, Laganiere S, Pascual-Leone A, et al. Finding the imposter: brain connectivity of lesions causing delusional misidentifications. Brain. 2016; 140(pt 2):1–11.
22. Fischer DB, Boes AD, Demertzi A, et al. A human brain network derived from coma-causing brainstem lesions. Neurology. 2016; 87:2427–2434. [PubMed: 27815400]
23. Laganiere S, Boes AD, Fox MD. Network localization of hemichorea-hemiballismus. Neurology. 2016; 86:2187–2195. [PubMed: 27170566]
24. Horn A, Kühn AA, Merkl A, et al. Probabilistic conversion of neurosurgical DBS electrode coordinates into MNI space. Neuroimage. 2017; 150:395–404. [PubMed: 28163141]
25. Fox MD, Buckner RL, White MP, et al. Efficacy of transcranial magnetic stimulation targets for depression is related to intrinsic functional connectivity with the subgenual cingulate. Biol Psychiatry. 2012; 72:595–603. [PubMed: 22658708]
26. Horn A, Kühn AA. Lead-DBS: a toolbox for deep brain stimulation electrode localizations and visualizations. Neuroimage. 2015; 107:127–135. [PubMed: 25498389]
27. McIntyre CC, Grill WM, Sherman DL, Thakor NV. Cellular effects of deep brain stimulation: model-based analysis of activation and inhibition. J Neurophysiol. 2004; 91:1457–1469. [PubMed: 14668299]
28. Åström M, Diczfalusy E, Martens H, Wårdell K. Relationship between Neural Activation and Electric Field Distribution during Deep Brain Stimulation. IEEE Trans Biomed Eng. 2015; 62:664–672. [PubMed: 25350910]
29. Ewert S, Plettig P, Li N, Chakravarty MM, Collins DL, Herrington TM, et al. Toward defining deep brain stimulation targets in MNI space: A subcortical atlas based on multimodal MRI, histology and structural connectivity. NeuroImage. 2017; doi: 10.1016/j.neuroimage.2017.05.015
30. Vorwerk J, Cho J-H, Rampp S, et al. A guideline for head volume conductor modeling in EEG and MEG. Neuroimage. 2014; 100:590–607. [PubMed: 24971512]
31. Hemm S, Mennessier G, Vayssiere N, et al. Co-registration of stereotactic MRI and isofieldlines during deep brain stimulation. Brain Res Bull. 2005; 68:59–61. [PubMed: 16325005]
32. Yeo BTT, Krienen FM, Sepulcre J, et al. The organization of the human cerebral cortex estimated by intrinsic functional connectivity. J Neurophysiol. 2011; 106:1125–1165. [PubMed: 21653723]
33. Horn A, Ostwald D, Reisert M, Blankenburg F. The structural-functional connectome and the default mode network of the human brain. Neuroimage. 2014; 102(pt 1):142–151. [PubMed: 24099851]
34. Horn A, Blankenburg F. Toward a standardized structural-functional group connectome in MNI space. Neuroimage. 2016; 124(pt A):310–322. [PubMed: 26327244]
35. Horn A, Neumann W-J, Degen K, Schneider G-H, Kühn AA. Toward an electrophysiological "sweet spot" for deep brain stimulation in the subthalamic nucleus. Human Brain Mapping. 2017; doi: 10.1002/hbm.23594
36. van Albada SJ, Robinson PA. Transformation of arbitrary distributions to the normal distribution with application to EEG test-retest reliability. J Neurosci Methods. 2007; 161:205–211. [PubMed: 17204332]
37. Mayberg HS, Lozano AM, Voon V, et al. Deep brain stimulation for treatment-resistant depression. Neuron. 2005; 45:651–660. [PubMed: 15748841]
38. Muthuraman M, Deuschl G, Koirala N, et al. Effects of DBS in parkinsonian patients depend on the structural integrity of frontal cortex. Sci Rep. 2017; 7:43571. [PubMed: 28262813]
39. Baudrexel S, Witte T, Seifried C, et al. Resting state fMRI reveals increased subthalamic nucleus–motor cortex connectivity in Parkinson's disease. Neuroimage. 2011; 55:1728–1738. [PubMed: 21255661]

40. Hanajima R, Ashby P, Lozano AM, et al. Single pulse stimulation of the human subthalamic nucleus facilitates the motor cortex at short intervals. J Neurophysiol. 2004; 92:1937–1943. [PubMed: 15152016]
41. Shirota Y, Ohtsu H, Hamada M, et al. Supplementary motor area stimulation for Parkinson disease: a randomized controlled study. Neurology. 2013; 80:1400–1405. [PubMed: 23516319]
42. Brys M, Fox MD, Agarwal S, et al. Multifocal repetitive TMS for motor and mood symptoms of Parkinson disease: a randomized trial. Neurology. 2016; 87:1907–1915. [PubMed: 27708129]
43. Ruffini G, Fox MD, Ripolles O, et al. Optimization of multifocal transcranial current stimulation for weighted cortical pattern targeting from realistic modeling of electric fields. Neuroimage. 2014; 89:216–225. [PubMed: 24345389]
44. Ellis T-M, Foote KD, Fernandez HH, et al. Reoperation for suboptimal outcomes after deep brain stimulation surgery. Neurosurgery. 2008; 63:754–760. discussion 760–761. [PubMed: 18981887]
45. Papapetropoulos S, Ellul J, Argyriou AA, et al. The effect of depression on motor function and disease severity of Parkinson's disease. Clin Neurol Neurosurg. 2006; 108:465–469. [PubMed: 16150537]
46. Jaggi JL, Umemura A, Hurtig HI, et al. Bilateral stimulation of the subthalamic nucleus in Parkinson's disease: surgical efficacy and prediction of outcome. Stereotact Funct Neurosurg. 2004; 82:104–114. [PubMed: 15305083]
47. Zaidel A, Bergman H, Ritov Y, Israel Z. Levodopa and subthalamic deep brain stimulation responses are not congruent. Mov Disord. 2010; 25:2379–2386. [PubMed: 20824733]
48. Butson CR, Cooper SE, Henderson JM, et al. Probabilistic analysis of activation volumes generated during deep brain stimulation. Neuroimage. 2011; 54:2096–2104. [PubMed: 20974269]
49. Howell B, McIntyre CC. Analyzing the tradeoff between electrical complexity and accuracy in patient-specific computational models of deep brain stimulation. J Neural Eng. 2016; 13:036023. [PubMed: 27172137]
50. Eisenstein SA, Koller JM, Black KD, et al. Functional anatomy of subthalamic nucleus stimulation in Parkinson disease. Ann Neurol. 2014; 76:279–295. [PubMed: 24953991]
51. Schmitz-Hubsch, T., Schneider, G-H., Horn, A., Krause, P., Gruber, D., Nickels, E., et al. The caudal zona incerta does not prove suitable as a target for deep brain stimulation in Parkinson's disease. Presented at the International Parkinson and Movement Disorder Society MDS; San Diego. 2014. p. 12

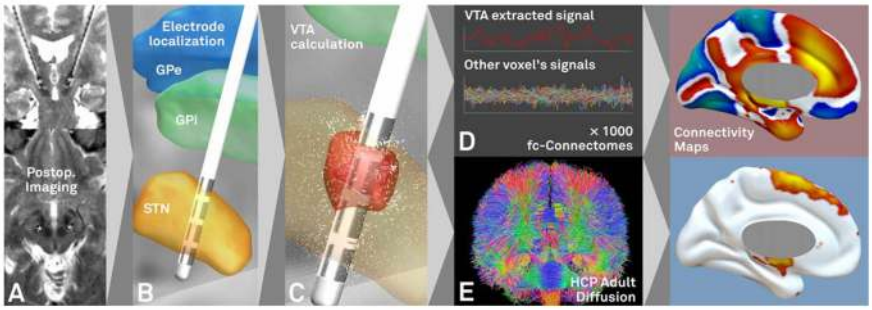

FIGURE 1.

Method for identifying deep brain stimulation (DBS) connectivity. Processing steps include acquiring pre-/postoperative imaging (A), localizing DBS electrodes in standard space (B), calculating the volume of tissue activated (VTA) based on stimulation parameters (C), then calculating functional (D) and structural (E) connectivity from the VTA to the rest of the brain using high-quality normative connectome data. Our processing stream using the connectome datasets defined in healthy subjects is shown and was used in all primary analyses. For functional connectivity, positive correlations are shown in warm colors whereas negative correlations (anticorrelations) are shown in cool colors (color version available online). GPe = globus pallidus externus; GPi = globus pallidus internus; HCP = Human Connectome Project; STN = subthalamic nucleus.

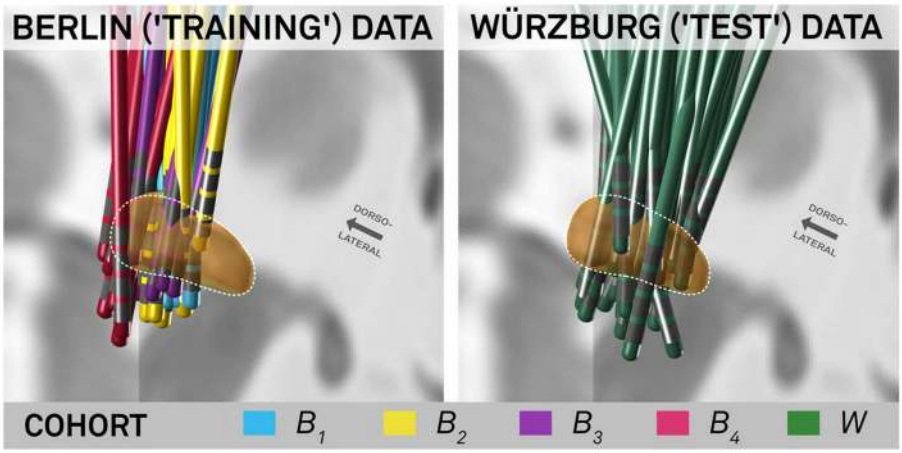

FIGURE 2.

Deep brain stimulation electrode localization and cohort information of training and test dataset. The Berlin dataset shown on the left ($B_{1–4}$) was used for training and cross-validation (applying a leave-one-subcohort-out design). The final model was then confirmed by applying it to the Würzburg test dataset (W, right).

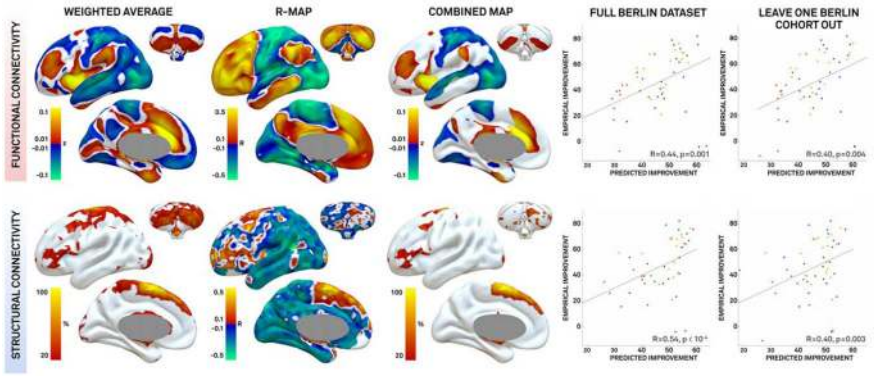

FIGURE 3.

Connectivity predictive of clinical improvement in the Berlin training dataset. Results from analyses using the connectome defined in healthy subjects are shown. Functional connectivity (top row) and structural connectivity (bottom row) associated with clinical improvement were identified using a weighted average (first column), correlation with clinical outcome (R maps, second column), and a combination of these two maps (third column). Using the combined map, clinical outcome was predicted for each patient using the full dataset (fourth column) and leave-one-cohort-out design (last column). Dot color (color version available online) represents subcohorts as specified in Figure 2.

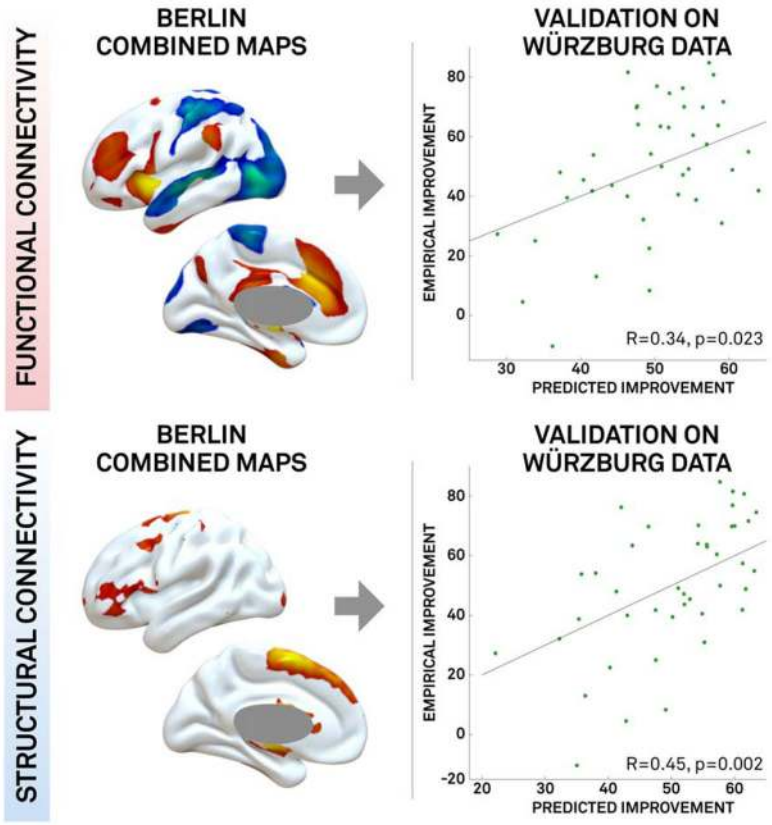

FIGURE 4.

Validation of connectivity profiles on an independent dataset. Connectivity maps generated using the Berlin training dataset (B_{1-4} combined) for both functional connectivity (top row) and structural connectivity (bottom row) predict clinical outcome in the independent Würzburg dataset.

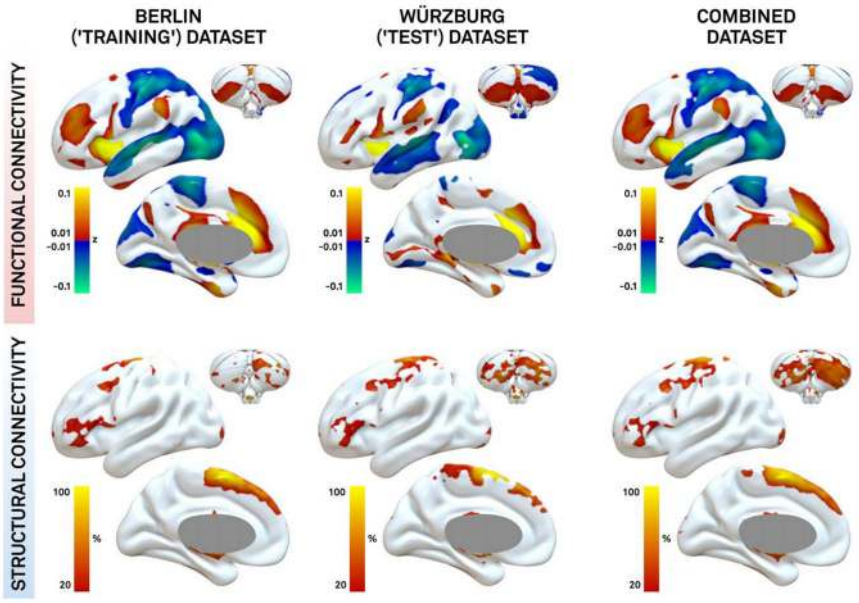

FIGURE 5.

The topography of connectivity associated with clinical response is consistent across datasets. Combined maps (weighted average and R map) are based on the Berlin dataset (left), Würzburg dataset (middle), and both datasets together (right).

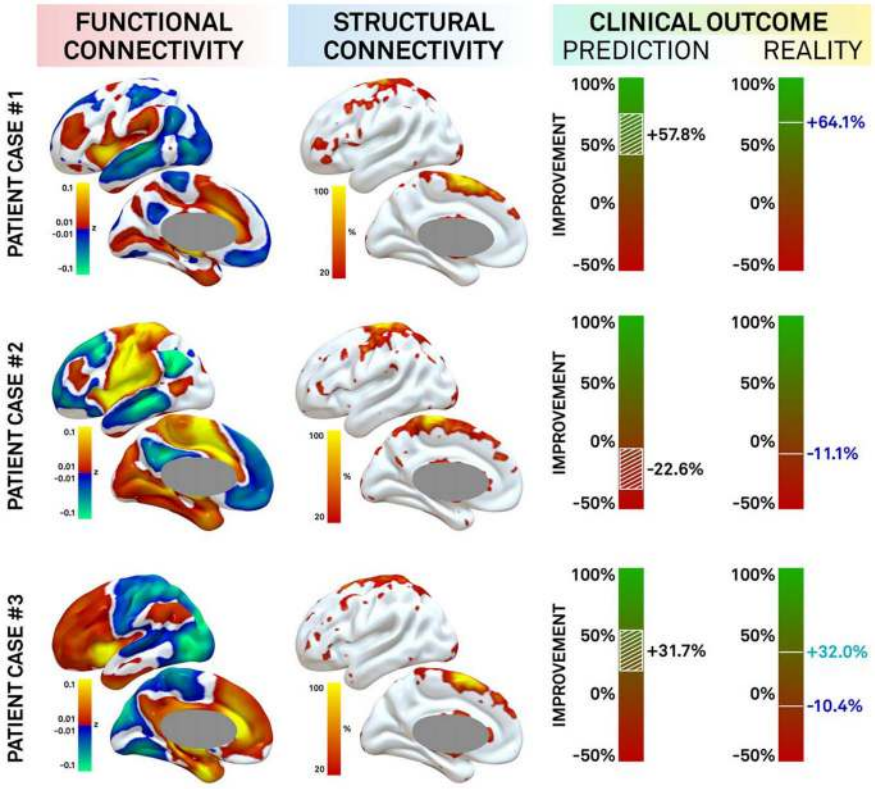

FIGURE 6.

Clinical outcome prediction in individual patients based on deep brain stimulation (DBS) connectivity. Connectivity between individual DBS sites and the rest of the brain is shown for 3 patients using functional connectivity (left) and structural connectivity (middle). Clinical response (right) was predicted based on the match of each patient's connectivity profile to that associated with good DBS response. Selected examples include a good responder with accurate prediction (top), a poor responder with accurate prediction (middle), and a poor responder with inaccurate prediction at the primary endpoint (+32%; bottom) who later improved to match our prediction with treatment of depression (−10.4%).

TABLE

Patient Demographics of All Cohorts and Subcohorts Analyzed

Cohort/ Subcohort	DBS Center	No. (female)	Age, yr	Disease Duration, yr	UPDRS-III Baseline, OFF Medication	L-dopa Response, %	Clinical Assessment	UPRDS-III Improvement, OFF Medication, %	LEDD Reduction, %	Postop Imaging	Related Citations
B	Berlin	51 (18)	60.0 ± 7.9	10.4 ± 3.9	38.6 ± 12.9	53.5 ± 17.2	ON vs OFF stim at 1–2 years postop	45.3 ± 23.0	52.8 ± 41.6	MRI, n = 45; CT, n = 6)	—
B_1		16 (9)	53.6 ± 5.5	9.8 ± 3.2	41.4 ± 14.5	54.5 ± 17.9		55.1 ± 15.7	74.9 ± 28.0		Schuepbach 2013[1]
B_2		11 (5)	66.1 ± 4.8	10.8 ± 4.1	36.4 ± 12.8	48.3 ± 19.3		37.2 ± 22.3	45.6 ± 36.3		—
B_3		12 (1)	59.8 ± 7.7	10.8 ± 4.8	37.2 ± 9.7	57.2 ± 15.1		54.9 ± 24.0	54.6 ± 30.4		Schmitz-Hubsch 2014[51]
B_4		12 (3)	63.1 ± 7.5	10.5 ± 3.9	38.1 ± 13.9	53.9 ± 18.7		30.1 ± 22.0	25.8 ± 57.3		
W	Wurzburg	44 (12)	60.4 ± 8.2	12.6 ± 4.5	49.6 ± 13.6	61.8 ± 18.4	Preop vs ON stim postop at 6–12 months	49.3 ± 24.8	61.4 ± 25.1	CT	—

Average values ± standard deviation are reported.

CT = computed tomography; DBS = deep brain stimulation; LEDD = L-dopa equivalent dose; MRI = magnetic resonance imaging; Postop = postoperative; Preop = preoperative; stim = stimulation; UPRDS = Unified Parkinson Disease Rating Scale.